Orthogonalized human protease control of secreted signals

Carlos A. Aldrete[†,1], Connor C. Call[†,1], Lucas E. Sant'Anna[2], Alexander E. Vlahos[1], Jimin Pei[3], Qian Cong[3,4,5], and Xiaojing J. Gao[1]

† These authors contributed equally to this work.
1 Department of Chemical Engineering, Stanford University, Stanford CA 94305, USA
2 Department of Bioengineering, Stanford University, Stanford CA 94305, USA
3 Eugene McDermott Center for Human Growth and Development, University of Texas Southwestern Medical Center, Dallas, TX 75390, USA
4 Department of Biophysics, University of Texas Southwestern Medical Center, Dallas, TX 75390, USA
5 Harold C. Simmons Comprehensive Cancer Center, University of Texas Southwestern Medical Center, Dallas, TX 75390, USA

Abstract

Synthetic circuits that regulate protein secretion in human cells could support cell-based therapies by enabling control over local environments. While protein-level circuits enable such potential clinical applications, featuring orthogonality and compactness, their non-human origin poses a potential immunogenic risk. Here, we developed Humanized Drug Induced Regulation of Engineered CyTokines (hDIRECT) as a platform to control cytokine activity exclusively using human-derived proteins. We sourced a specific human protease and its FDA-approved inhibitor. We engineered cytokines (IL-2, IL-6, and IL-10) whose activities can be activated and abrogated by proteolytic cleavage. We utilized species specificity and re-localization strategies to orthogonalize the cytokines and protease from the human context that they would be deployed in. hDIRECT should enable local cytokine activation to support a variety of cell-based therapies such as muscle regeneration and cancer immunotherapy. Our work offers a proof of concept for the emerging appreciation of humanization in synthetic biology for human health.

Intercellular communication, mediated by the secretion and display of soluble factors (cytokines and growth factors) and receptors, plays a crucial role in health and diseases. Cell therapies aim to treat complex diseases using human cells through the modulation of intercellular communication[1], with the chimeric antigen receptor (CAR) T cell therapy being the most notable example[2]. Aside from treating cancer, other promising examples are the treatment of autoimmune diseases and supporting muscle regeneration using mesenchymal stem cells (MSCs)[3–6]. Despite their promise, many cellular therapeutics are susceptible to changes in the local microenvironment[7–9]. To address this hurdle, researchers have "armed" cell therapies to constitutively secrete cytokines to tune their local environments to promote proliferation and efficacy, such as driving CAR-T activation in solid tumors using IL-12[10], and improving the survival of transplanted MSCs using the anti-inflammatory IL-10[11]. While constant expression of these powerful signals improve efficacy, increased toxicity was also observed, indicating a need for further control[10].

The field of synthetic biology offers a plethora of tools and methods for localized, conditional control of cytokine activity. In particular, compared to the more conventional transcriptional control, protein-level controls hold advantages for potential clinical use such as fast operation, compact single-transcript delivery, and context-independent performance[12]. Notably, orthogonal viral proteases have emerged as useful post-translational tools due to their ability to control the activity, degradation, and localization of target proteins with high substrate specificity[13,14]. These orthogonal proteases are highly versatile and can be combined to implement robust sense-and-response behaviors in mammalian cells. They are uniquely positioned to serve as cargos on mRNA vectors that are safer and more scalable than conventional DNA vectors[15]. Moreover, they have been successfully applied to the control of protein secretion and display[16,17].

However, despite the promise of proteases as control knobs, there remains a critical constraint: the non-human origin and potential immunogenicity of viral proteases may preclude their translational potential. In analogous scenarios, immune responses against other synthetic biology tools such as *Streptococcus pyogenes* Cas9 protein (SpCas9) and synthetic CAR-T receptors have been documented with compromised efficacy and duration, highlighting the need to reduce immunogenicity of synthetic tools[18,19]. Even more notably, we are inspired by the decades of efforts to "humanize" monoclonal antibodies[20,21], and we reason that, if synthetic biology is to deliver its promise in human health, it is imperative that we preempt similar challenges as we engineer the fundamental tools. In an emerging consensus to "humanize" synthetic biology, groups have developed tools derived largely from human-derived components such as zinc finger transcriptional regulators (synZiFTRs)[22], CRISPR-CAS-inspired RNA targeting systems (CIRTS)[23], and synthetic intramembrane proteolysis receptors (SNIPRs)[24]. While these papers have demonstrated humanized transcriptional and translational regulation, the humanization efforts have yet to reach the post-translational level.

Here, we sought to develop protease-based control of intercellular communication for potential application in cellular therapeutics. We developed our system with five features for potential clinical suitability, combining general humanization considerations[22] with the unique benefits of protease control: (i) use of human-derived proteins to minimize the risk of immunogenicity; (ii) use of orthogonalized components with high specificity and minimal crosstalk with native signaling pathways; (iii) ability to control exogenously using FDA-approved small molecules; (iv) compact, single-transcript design to facilitate delivery into

therapeutic cells; (v) compatibility with mRNA delivery for potential transient *in vivo* delivery applications.

We identified a human protease involved in blood pressure regulation, renin, as the control knob. Renin, in contrast to most human proteases, exhibits high substrate specificity[25]. Additionally, renin comes with a clinically-viable mode of exogenous control in the form of its FDA-approved small-molecule inhibitor, aliskiren[26]. In contrast to previously used cytosolic viral proteases, renin functions extracellularly and in the secretory pathway, offering an external interface to directly control intercellular communication.

In this paper, we introduce Humanized Drug Induced Regulation of Engineered CyTokines (hDIRECT), using renin to control intercellular communication. We engineered a variety of clinically relevant cytokines (IL-2, IL-6, and IL-10), whose activities are increased or decreased by renin-mediated proteolysis and can be tuned exogenously via aliskiren. We used structure-guided mutagenesis and re-localization strategies to create renin mutants with new and orthogonal substrate specificity from wildtype proteins. Finally, we demonstrate chemically dependent and bidirectional control of simultaneous cytokine activity, compact delivery using various methods and in multiple cell types, as well as small-molecule control *in vivo*. We envision that conditional control of cytokine activity has immediate use for supporting and controlling cell therapies as well as dissecting biological functions of dynamic cytokine profiles – because most of the specific protease-regulated cytokine designs are reported for the first time in this study. This study demonstrates a proof-of-principle for the orthogonalization of human proteases and serves as an example of making biomolecular controls more clinically compatible.

Results

Engineering caged cytokines.

hDIRECT consists of three components: a membrane-bound renin, renin's FDA-approved small-molecule inhibitor, aliskiren, and engineered cytokines modulated by renin cleavage (Fig. 1a, b). Renin is known to function extracellularly as it is natively secreted by juxtaglomerular cells in the kidney[25]. To localize renin to the plasma membrane to enable the autonomous control of engineered cells, the active form of renin was fused to the transmembrane domain of human CD28 (Fig. 1b). Here, constitutive expression of membrane-bound renin can control the activity of co-expressed secreted cytokines. We first evaluated a variety of strategies to place cytokines under the control of renin.

To engineer cytokines activated by renin cleavage, we drew inspiration from previous work on attenuated cytokines, specifically, receptor-masked interleukin-2 (IL-2).[27,28] Here, IL-2 activity was tied to proteolytic cleavage by fusing IL-2 with a receptor subunit via a matrix metalloproteinase (MMP)-cleavable linker. Cytokine activity is inhibited ("caged") in the absence of protease, and conditionally activated ("uncaged") by proteolytic cleavage. Using this general framework, we demonstrated the possibility to cage structurally and functionally distinct cytokines. Inspired by MSC and CAR T applications, we chose interleukin-10 (IL-10, an immuno-suppressive cytokine that plays a role in limiting host immune responses as well as promoting wound healing and muscle regeneration[29]), interleukin-6 (IL-6, generally associated with inflammation, but also implicated with the activation of satellite cells and promotion of myotube regeneration for muscle regeneration[30–32]), and IL-2 (a potent factor for the proliferation and activation of lymphocytes, and widely studied for activating effector T cells against tumors[33–35]).

We started by designing a caged IL-10. IL-10 is composed of a homodimer that binds to a tetrameric IL-10 receptor complex formed by two IL-10Ra and two IL-10Rb subunits.[36] Since effectively caging a dimeric protein may be difficult due to having multiple epitopes to interact with receptors, we also tested a previously engineered monomeric variant of IL-10 (R5A11M) with boosted affinity for IL-10Rb and potent immunomodulatory effects.[37] We created two caged IL-10 constructs. Both designs contain a renin cleavable linker (cut site and glycine-serine, GS, linker) and the extracellular portion of specific IL-10R subunits for caging. The first construct was created by fusing two WT IL-10 monomers together with IL-10Ra (CageIL-10-dimer – Fig. 1a). The second construct used the monomeric R5A11M IL-10 and IL-10Rb (CageIL-10-mono – Fig. 1a). We hypothesized that aliskiren could be used to control renin activity and removal of the caged portion of hDIRECT to control cytokine activity (Fig. 1b).

Taking advantage of our fast design-build-test cycle, we transiently transfected human embryonic kidney (HEK) 293 cells using plasmids encoding the caged cytokines and renin. Supernatant was transferred to HEK-Blue™ IL-10 reporter cells to assess functional activity. Here, signal transduction from IL-10 receptor activation results in expression of secreted embryonic alkaline phosphatase (SEAP), which can be assayed via absorbance following incubation with a colorimetric substrate. A schematic for this cytokine reporter assay can be found in Supplementary Fig. 1 and links to plasmid maps as well as amounts of plasmid for each transient transfection can be found in Supplementary Tables 1 and 2. Unless specified otherwise, the same workflow for the cytokine reporter assay was used throughout this work. In the absence of renin, cageIL-10-mono was caged more efficiently than the cageIL-10-dimer (Fig. 1c). CageIL-10-mono was also able to fully reconstitute activity with protease present (Fig. 1c). From here on, we refer to this optimal variant as "cageIL-10". Next, to explore the extent of IL-10 caging and linker cleavability, we titrated the amount of transfected cageIL-10 plasmid DNA. We observed efficient caging even at high doses of cageIL-10 (Fig. 1d), and renin-activated IL-10 activity at low doses of cageIL-10 (Fig. 1d). We then validated that aliskiren enables dose-dependent control of hDIRECT (Fig. 1e) at therapeutically relevant concentrations <500 nM[26]. Decreasing the amount of renin plasmid increased the sensitivity of the system to aliskiren (Supplementary Fig. 2). Western blot analysis confirms cageIL-10 cleavage by renin and inhibition by aliskiren (Supplementary Fig. 3a).

To expand the cytokine output of hDIRECT, we next developed caged designs for IL-6. Structurally, IL-6 is a monomeric four-α helical bundle typical of most cytokines (distinct from the dimeric IL-10). Canonically, IL-6 binds to its high affinity receptor, IL-6Ra, on cell surfaces, followed by complexing on the membrane with IL-6Rb (gp130) which transduces signal activation across the membrane[38]. However, IL-6 activity has also been implicated in an alternative pro-inflammatory pathway wherein IL-6 binds to soluble IL-6Ra (sIL-6Ra) and mediates transactivation on cells expressing IL-6Rb[39]. To avoid transactivation of our caged IL-6 complex and bias IL-6 signaling to a regenerative phenotype, we sought to cage IL-6 with an IL-6Ra mutant (A228D/N230D/H280S/D281V) that has abrogated activation of IL-6Rb. We denote this IL-6Ra mutant as IL6Ra_M4.

Inspection of the IL-6-receptor complex structures suggested that placing IL-6Ra at the N-terminus of the fusion protein would allow IL-6 to bind IL-6Ra in its canonical conformation. Consistent with this observation, our data shows improved caging when the receptor is fused to the N-terminus, although fusion at either terminus exhibits substantial renin-independent activation (Supplementary Fig. 4). We hypothesized that caging could be improved if we fused an additional receptor subunit. Therefore, we created a multi-cageIL-6 by fusing IL-6Ra_M4 to

167 the N-terminus and IL-6Rb to the C-terminus of IL-6 with renin-cleavable linkers (Fig. 2a).
168 Indeed, multi-cageIL-6 demonstrated vastly improved caging over the initial design (Fig. 2b),
169 albeit with reduced activity in the presence of renin (Fig. 2b). However, we found that IL-6
170 activity in response to renin can be increased at higher doses of multi-cageIL-6 plasmid (Fig. 2c).
171 Finally, to show broad generalizability in cytokines and therapeutic applications, we
172 ported over previous caged IL-2 constructs to hDIRECT[27]. A mutant IL-2 (sumIL-2) was
173 recently developed with enhanced affinity for IL-2Rb (i.e., effector T cells) over IL-2Ra (i.e.,
174 regulatory T cells)[28]. We leveraged this insight to design a caged sumIL-2 with a renin-cleavable
175 linker and C-terminal IL-2Rb (Fig. 2d). We also investigated whether varying the linker length
176 on either side of the renin cut site would improve cleavability but did not find any significant
177 effect (Supplementary Fig. 5). CageIL-2 is efficiently caged at high doses of cytokine (Fig. 2e)
178 and exhibits renin-activation at low doses (Fig. 2e). IL-2 activity was tuned sensitively by
179 aliskiren upon drug titration (Fig. 2f), indicating that aliskiren control is also generalizable
180 between different cytokines. Altogether, we established three different caged cytokines
181 compatible with renin-aliskiren control.
182
183 **Engineering cleavable cytokines.**
184 To expand the potential of protease regulation, we sought to design cytokines whose
185 activities would be abrogated (rather than activated) by cleavage. Compared to the caged design,
186 this modality would allow cytokine activity to be "turned on" or restored by a small-molecule
187 input. It could be particularly useful in applications where temporary, rather than constitutive,
188 cytokine activity is desired, such as transient IL-2 activation to support CAR-T cell proliferation
189 and cytotoxicity while avoiding exhaustion and overstimulation[40].
190 We hypothesized that cytokines could be directly inactivated if they were engineered to
191 include protease cut sites. We inserted protease cut sites within flexible loops of cytokines so as
192 not to perturb receptor binding regions. Like the caged cytokines, we envision engineered cells
193 constitutively expressing cleavable cytokines and membrane-bound renin. In this fashion,
194 cytokine activity can be tuned up on demand upon drug input and protease inhibition (Fig. 3a).
195 We started designing cleavable cytokines using the previously mentioned mono-IL-10.
196 Researchers engineered this functional mono-IL-10 by inserting a flexible, 6 amino acids,
197 GGGSGG linker between the D and E helices of human IL-10[37]. We leveraged this insight to
198 create a cleavable mono-IL-10 by replacing this glycine linker with the 13 amino acid renin
199 cleavage site. CleaveIL-10 retained activity in the absence of protease and was abrogated upon
200 co-transfection with renin (Fig. 3b). To explore the range at which cleaveIL-10 is sensitive to
201 renin cleavage, we co-transfected cells with or without renin while titrating the amount of
202 cleaveIL-10 DNA and observed a substantial shift of the titration curves by renin (Fig. 3c).
203 Next, we sought to demonstrate the generalizability of this method to native cytokines
204 that lack synthetic linkers to substitute. Our general method was to find sites in human IL-6 and
205 IL-2 tolerable (retaining activity) to insertion of a protease cut site. We scanned various solvent
206 exposed (protease accessible) flexible loops between helices to find tolerable insertions
207 (Supplementary Fig. 6) and then optimized linkers to improve their cleavability. Cleave IL-6 and
208 IL-2 were designed through direct insertion of the renin cut site with or without a five amino acid
209 GS linker into flexible loops at residues 127-140 in IL-6 and 74-81 in IL-2. Both cleaveIL-6
210 (Fig. 3d) and cleaveIL-2 (Fig. 3e) retained their functional activity in the absence of protease.
211 Additionally, we observed substantial shifts in response to renin in both cleaveIL-6 (Fig. 3d) and
212 cleaveIL-2 (Fig. 3e).

To demonstrate that this cleavable method can be used to turn on cytokine activity by a small-molecule input, we determined that cleaveIL-10 activity can be tuned via aliskiren (Fig. 3f). Western blot analysis also confirms the cleavage of cleaveIL-10 by renin and inhibition by aliskiren (Supplementary Fig. 3b). Taken together, these results demonstrate successful engineering of cleavable cytokine constructs for three structurally distinct cytokines also compatible with renin-aliskiren control.

Orthogonalization of hDIRECT from its human counterparts.

After establishing renin-regulated secreted cytokines, our next goal was to orthogonalize the system from human hosts. In contrast to parts sourced from other organisms (e.g., viral proteases), utilizing human parts bears the distinct and critical risk of off-target effects due to crosstalk with other human proteins. In particular, renin is endogenously secreted into the blood to regulate blood pressure via proteolytic cleavage of angiotensinogen[25]. Therefore, to avoid crosstalk with the host, there are two issues to address: the activation of angiotensinogen by cell-surface, exogenous renin and the cleavage of engineered cytokines by endogenous renin.

To address the first problem, we took inspiration from our previous work and hypothesized that we could spatially separate renin from circulation by localizing it to the endoplasmic reticulum (ER) of the engineered cell[16,41]. We fused renin to the CD4 transmembrane domain and a cytosolic ER-retention motif (RXR). Here, renin regulates engineered cytokines in cis as the cytokines move through the secretory pathway, while remaining sequestered from renin's endogenous substrate in the blood (Fig. 4a). Using cageIL-10 as a test case, we validated that ER-retained renin maintained the ability to activate secreted cageIL-10 (Fig. 4b). Next, to ensure that aliskiren could permeate engineered cells and inhibit ER-renin with a similar sensitivity (as it typically acts extracellularly), we performed aliskiren titration and validated that ER-renin retains aliskiren sensitivity (Fig. 4c).

To address the second problem of endogenous renin cleaving the engineered cytokines, we took inspiration from renin's diversity of specificities across species. In particular, human and mouse angiotensinogen are not recognized by the opposing renins[42]. We hypothesized that we could use the mouse cut site in engineered cytokines to avoid their cleavage by circulating human renin, and in parallel minimally engineer human renin to recognize the mouse site such that the protease is still unlikely to be recognized as non-human. To introduce mouse substrate recognition, we compared substrate bound renin structures across species. Compared to human renin, mouse renin has a larger binding pocket to accommodate bulkier substrate residues (L35 and Y36). We hypothesized that by mutating four substrate-binding residues in human renin to corresponding residues in mouse renin with smaller side chains (L147I, R148H, I203V, L290V) we could expand the binding pocket to accommodate the mouse substrate. We denote this mutant renin as human-to-mouse (H2M) renin. A more detailed structural analysis can be found in Supplementary Fig. 7. We then tested the orthogonality of the renin protease and found that the human and mouse renins only recognize their corresponding cut sites while the H2M renin's specificity is expanded to recognize both (Fig. 4d). We confirmed that H2M, ER-localized renin remains sensitive to aliskerin (Fig. 4e) and that ER-localization does not affect orthogonality (Fig. 4f).

In summary, human renin was successfully orthogonalized using structure-guided mutation and localization motifs. Importantly, these orthogonalization strategies did not compromise renin function or sensitivity to aliskiren. We expect that ER-retained H2M renin and

258 caged and cleavable cytokines harboring the mouse cut site will have minimal crosstalk with
259 endogenous human renin and angiotensinogen.
260
261 **Therapeutically relevant applications of hDIRECT in mammalian cells.**
262 Clinically, *ex vivo* gene delivery to engineer therapeutic cells is bottlenecked by viral
263 packaging limits of ~5 kb (adeno-associated virus) to ~10 kb (lentivirus)[43,44]. Compact genetic
264 constructs are therefore a critical requirement for translational applications. To demonstrate that
265 hDIRECT enables compact delivery, we created single-transcript constructs encoding engineered
266 cytokines and renin separated by 2A "self-cleaving" peptides[45].
267 We created a polycistronic construct containing cageIL-10 (mRens), ER-retained H2M
268 renin, and a fluorescent co-transfection marker, mCherry (Fig. 5a). Transient transfection of this
269 construct in HEK293 cells enables inhibition of IL-10 activity upon dosing with aliskiren, albeit
270 with reduced aliskiren sensitivity (Fig. 5a). We hypothesize this reduced sensitivity could be due
271 to overexpression of the renin protease, as had been seen in Supplementary Fig. 2. While it is
272 difficult to fine tune protein ratios in a polycistronic construct, we hypothesize methods to reduce
273 overall protein levels will improve aliskiren sensitivity, such as controlling the number of
274 genomic integrations or number of cells delivered. Next, we sought to demonstrate simultaneous
275 control over the activities of multiple cytokines, as immune and regenerative responses are often
276 mediated by a variety of cytokine signals with characteristic dosing and temporal profiles.[46,47]
277 For example, muscle regeneration is mediated by an initial pro-inflammatory regime (i.e. IL-6),
278 stimulating and recruiting the innate immune system, followed by an anti-inflammatory regime
279 (i.e. IL-10) to indirectly promote the differentiation of muscle stem cells.[48] To demonstrate that
280 hDIRECT can simultaneously control the activity of multiple cytokines, we created single-
281 transcript constructs containing both cageIL-10 and cleaveIL-6 (Fig. 5b) to mimic a cytokine
282 response for promoting muscle regeneration. In this manner, delivery with drug should allow an
283 initial regime of IL-6 activity, followed by a switch to IL-10 activity when drug is removed.
284 HEK293 cells transiently transfected with this single-transcript construct demonstrated
285 bidirectional control of IL-10 and IL-6 activity with aliskiren (Fig. 5b).
286 Next, we tested whether hDIRECT's performance is robust against different delivery
287 methods or cellular contexts. First, we created lentiviral constructs using a weaker constitutive
288 promoter, EF1-α, to potentially improve the aliskiren sensitivity of the polycistronic cageIL-10
289 design (from Fig. 5a). Indeed, stable transduction of HEK293 cells enabled regulation of IL-10
290 activity with improved aliskiren sensitivity (Fig. 5c). Additionally, we observed greater aliskiren
291 sensitivity at lower seeding densities of stably transduced cells (Supplementary Fig. 9). We also
292 conducted kinetic experiments of stable cageIL-10 cells to characterize the induction and
293 reversibility with aliskiren (Supplementary Fig. 10). Next, we sought to test hDIRECT in another
294 cell line to validate its generalizability to different cell types. We chose Jurkat cells as an
295 accessible proof of concept model for regulating IL-2 activity in the context of a CAR-T cell
296 therapy. We designed lentiviral constructs using the EF1-α promoter and a polycistronic cageIL-
297 2 design (Fig. 5d). Stably transduced Jurkats exhibited lower levels of secretion compared to
298 HEK293s but retained high sensitivity to aliskiren (Fig. 5d). To assess whether the level of
299 cytokine activities from our cells were therapeutically relevant, we conducted a series of
300 recombinant cytokine titrations on the HEKBlue reporter cells (Supplementary Figure 11). IL-6
301 and IL-10 have been reported to promote muscle regeneration at 10 ng/mL, within the detection
302 range of their respective reporter cells[49,50]. Notably, the apparent uncaged IL-2 concentration
303 from the stably transduced Jurkat cells corresponds with a cytokine concentration of 20 ng/mL

304 which is sufficient to stimulate primary T cell expansion (2-15 ng/mL)[51]. We note that while this
305 reporter assay may not be suited for granular cytokine quantification, it does give a general
306 indication whether cytokine activities are at or below these relevant concentrations.
307 Finally, we sought to demonstrate whether hDIRECT could function in therapeutically
308 relevant contexts, as well as more precisely quantify cytokine levels using enzyme-linked
309 immunosorbent assays (ELISAs). One potential application for hDIRECT could local, aliskiren-
310 switchable stimulation of immune cells for immunotherapy. To demonstrate this, we stably
311 engineered K-562 cells using the cageIL-2 lentiviral construct from Fig. 5d, so that the K-562s
312 will switch off IL-2 activity in response to aliskiren. The hDIRECT K-562s were co-cultured
313 with primary T cells in IL-2 free media (Fig. 6a), and, indeed, we observed aliskiren-regulated T
314 cell proliferation in response to the hDIRECT K-562s (Fig. 6b). Similarly, quantification of
315 supernatant IL-2 levels demonstrated aliskiren-dependent IL-2 activity (Fig. 6c). We note that
316 uncaged IL-2 levels were higher than the 200 U/mL recombinant IL-2 control typically used in T
317 cell cultures, and the residual caged IL-2 levels probably contributed to the proliferation in the
318 aliskiren– condition. The latter could be further tuned in the future by decreasing the number of
319 engineered cells delivered.
320 To further demonstrate hDIRECT's compact design and unqiue compatibility with
321 mRNA delivery for potential *in vivo* gene delivery applications, we synthesized an mRNA
322 transcript encoding the same cageIL-2 construct as above via *in vitro* transcription (Fig. 6d).
323 mRNA transfection of HEK293 cells with this construct retained therapeutically relevant
324 expression levels of IL-2 and aliskiren-dependent activity measured via ELISA (Fig. 6e).
325 To explore the potential for the core mechanism of hDIRECT to be tuned by aliskiren *in*
326 *vivo*, we conducted a pilot mouse study. We opted to use luciferase activity as a sensitive and
327 orthogonal output that can be easily measured from mouse sera. We developed a membrane-
328 tethered nanoluciferase that can be released by human renin, but not mouse renin, allowing for
329 aliskiren-regulated luciferase activity from engineered cells (Fig. 6f). To demonstrate aliskiren-
330 regulation *in vivo*, we used hydrodynamic gene delivery to introduce into the mouse liver
331 plasmids encoding membrane-bound renin-responsive luciferase, membrane-bound human renin,
332 and a constitutive co-secretion marker, SEAP, for signal normalization (Fig. 6g). Mice were
333 given 100 mg/kg doses of aliskiren via oral gavage 2 hours prior and after tail vein injection of
334 plasmids (Fig. 6h). Mice receiving aliskiren had reduced luciferase activity similar to that of the
335 negative control without renin expression (Fig. 6i).
336 These results demonstrate that hDIRECT can be delivered compactly using various
337 delivery methods and to multiple cell types, regulate cytokines at therapeutically relevant
338 concentrations, and be tuned exogenously *in vivo* through oral dosing of aliskiren.
339

340 **Discussion**

341 Here, we have presented a post-translational, humanized platform, hDIRECT, for drug-
342 mediated regulation of secreted cytokine activity in mammalian cells. Exclusively using human
343 proteins and domains, hDIRECT confers protease control with opposing signs ("caged" and
344 "cleavable") over cytokine activity. Co-expression of engineered cytokines renin allows the
345 control of cytokine activity using renin's FDA-approved inhibitor, aliskiren. We used species
346 specificity and re-localization strategies to orthogonalize both renin and engineered cytokines to
347 avoid crosstalk with their human counterparts. We showed that hDIRECT is compact and can
348 regulate the activities of multiple cytokines encoded on a single transcript in different
349 mammalian cells. Lastly, we demonstrated hDIRECT can control primary T cell proliferation, be

350 delivered compactly on an mRNA, and can be tuned via oral administration of aliskiren in mice.
351 hDIRECT therefore represents a proof-of-concept towards humanized engineering for post-
352 translational tools to control next-generation cell therapies.
353 While we have shown that hDIRECT can regulate cytokines, we expect that the
354 proteolytic control module can be extended to a variety of secreted and membrane proteins of
355 interest. Growth factors and chemokines, which regulate the proliferation, differentiation, and
356 migration of cells, could be similarly engineered for proteolytic regulation. In addition, we
357 envision that receptors with cleavable pro-domains or competitive caging domains might offer
358 small-molecule control of receptor availability which, for example, could tune the activity of
359 CAR-T cells to limit exhaustion[40].
360 We envision that hDIRECT will find immediate applications in cellular therapeutics.
361 hDIRECT could be used to temporarily supply CAR-T cells with IL-2 to improve proliferation
362 and cytotoxicity. In applications where the temporal profile of cytokine activity is critical, such
363 as MSC therapy for muscle regeneration, hDIRECT can be used to activate pro-inflammatory IL-
364 6 followed by regenerative, anti-inflammatory IL-10. While this work demonstrates the control
365 of two cytokines simultaneously, lentiviral packaging could allow for the delivery of a single
366 transcript encoding up to five engineered cytokines. hDIRECT could also be used for research in
367 basic science investigating the timing and dosage of various cytokine regimes by imparting
368 temporal control over the activity of multiple cytokines.
369 While our system is built from native human proteins, the presence of junctions from
370 fusion of domains and a small number of mutations introduced for improving function and
371 orthogonalization may still be recognized as foreign. Computational analysis of the ER-H2M
372 renin protein using peptide-MHC I binding and immunogenicity prediction algorithms[52,53]
373 confirmed that the protein contained less potentially immunogenic regions when compared with
374 commonly used viral proteases, TEVp and HCVp (Supplementary Fig. 12). While we note that
375 immunogenicity can only be definitively assessed in patients, *in vitro* assays, such as IFN-γ
376 ELISpots, can serve as a proxy to monitor donor T cell responses to antigenic peptides. Various
377 doses of a peptide pool containing all 9-mer peptides of the orthogonalizing H2M-renin
378 mutations did not elicit an immune response from T cells from any of the four healthy (HLA-
379 A*02:01) donors tested (Supplementary Fig. 13). Although this currently only assesses pre-
380 existing immunity, it could also be used to track acquired immunity in future patients. We
381 believe that this workflow can be used to screen, test, and iterate functional and immune-
382 tolerized portions over the rest of the junctions from the fusion of domains. We anticipate that
383 our humanization effort is a step towards immune-tolerized synthetic circuits.
384 While clinically suitable, hDIRECT still requires further work for potential use in
385 humans. Notably, most experiments here were conducted in the model mammalian cell line,
386 HEK293. Future work in primary cells more aligned with an intended clinical application, such
387 as CAR-T cells, could further demonstrate the functional efficacy of this platform. Subsequently,
388 *in vivo* experiments using mouse cytokines will help to determine the pharmacokinetics of small-
389 molecule dosing and localized cytokine activity in a more complex environment. It is important
390 to note that aliskiren has been shown to be tolerable and safe at oral doses of up to 600 mg in
391 healthy patients, including elderly[54,55]. This dose corresponds to a C_{max} of 300 ng/mL, which
392 relates to a drug concentration of 543 nM that we use to benchmark the sensitivity of
393 hDIRECT[26]. The most common adverse events reported at this dosing are headaches, dizziness,
394 and nausea but these occur at low incidence rates (1-5%) similar to placebo. To minimize side

395 effects, renin could be further engineered to be more sensitive to aliskiren so lower doses can be
396 used or the dose of cells delivered can be lowered.
397 In summary, hDIRECT is the first post-translational control platform using
398 orthogonalized humanized components in mammalian cells. Using hDIRECT, we demonstrate
399 small-molecule control of multiple secreted cytokines simultaneously, compact delivery using
400 various methods and in multiple cell types, as well as small-molecule control *in vivo*. We
401 envision that hDIRECT is generalizable towards a wide variety of extracellular factors and
402 receptors to tune them. Ultimately, we believe our novel engineered cytokines will facilitate
403 basic biology research by dynamically controlling cytokine activities, and the hDIRECT
404 platform holds the promise to enhance cell and gene therapies.
405

406 **References**

407 1. Fischbach, M. A., Bluestone, J. A. & Lim, W. A. Cell-based therapeutics: the next pillar
408 of medicine. *Sci. Transl. Med.* **5**, 179ps7 (2013).
409 2. Labanieh, L., Majzner, R. G. & Mackall, C. L. Programming CAR-T cells to kill cancer.
410 *Nat. Biomed. Eng.* **2**, 377–391 (2018).
411 3. Ninagawa, N. T. *et al.* Transplantated mesenchymal stem cells derived from embryonic
412 stem cells promote muscle regeneration and accelerate functional recovery of injured
413 skeletal muscle. *Biores. Open Access* **2**, 295–306 (2013).
414 4. Winkler, T. *et al.* Dose-response relationship of mesenchymal stem cell transplantation
415 and functional regeneration after severe skeletal muscle injury in rats. *Tissue Eng. Part A*
416 **15**, 487–492 (2009).
417 5. Munir, H. & McGettrick, H. M. Mesenchymal stem cell therapy for autoimmune disease:
418 risks and rewards. *Stem Cells Dev.* **24**, 2091–2100 (2015).
419 6. Squillaro, T., Peluso, G. & Galderisi, U. Clinical trials with mesenchymal stem cells: an
420 update. *Cell Transplant.* **25**, 829–848 (2016).
421 7. Marofi, F. *et al.* CAR T cells in solid tumors: challenges and opportunities. *Stem Cell*
422 *Res. Ther.* **12**, 81 (2021).
423 8. Preda, M. B. *et al.* Short lifespan of syngeneic transplanted MSC is a consequence of in
424 vivo apoptosis and immune cell recruitment in mice. *Cell Death Dis.* **12**, 566 (2021).
425 9. Kim, N. & Cho, S.-G. New strategies for overcoming limitations of mesenchymal stem
426 cell-based immune modulation. *Int. J. Stem Cells* **8**, 54–68 (2015).
427 10. Kerkar, S. P. *et al.* Tumor-specific CD8+ T cells expressing interleukin-12 eradicate
428 established cancers in lymphodepleted hosts. *Cancer Res.* **70**, 6725–6734 (2010).
429 11. Nitahara-Kasahara, Y. *et al.* Enhanced cell survival and therapeutic benefits of IL-10-
430 expressing multipotent mesenchymal stromal cells for muscular dystrophy. *Stem Cell*
431 *Res. Ther.* **12**, 105 (2021).
432 12. Chen, Z. & Elowitz, M. B. Programmable protein circuit design. *Cell* **184**, 2284–2301
433 (2021).
434 13. Gao, X. J., Chong, L. S., Kim, M. S. & Elowitz, M. B. Programmable protein circuits in
435 living cells. *Science* **361**, 1252–1258 (2018).
436 14. Fink, T. *et al.* Design of fast proteolysis-based signaling and logic circuits in mammalian
437 cells. *Nat. Chem. Biol.* **15**, 115–122 (2019).
438 15. Sahin, U., Karikó, K. & Türeci, Ö. mRNA-based therapeutics--developing a new class of
439 drugs. *Nat. Rev. Drug Discov.* **13**, 759–780 (2014).

16. Vlahos, A. E. *et al.* Protease-controlled secretion and display of intercellular signals. *Nat. Commun.* **13**, 912 (2022).
17. Praznik, A. *et al.* Regulation of protein secretion through chemical regulation of endoplasmic reticulum retention signal cleavage. *Nat. Commun.* **13**, 1323 (2022).
18. Ferdosi, S. R. *et al.* Multifunctional CRISPR-Cas9 with engineered immunosilenced human T cell epitopes. *Nat. Commun.* **10**, 1842 (2019).
19. Lamers, C. H. J. *et al.* Immune responses to transgene and retroviral vector in patients treated with ex vivo-engineered T cells. *Blood* **117**, 72–82 (2011).
20. Riechmann, L., Clark, M., Waldmann, H. & Winter, G. Reshaping human antibodies for therapy. *Nature* **332**, 323–327 (1988).
21. Jones, P. T., Dear, P. H., Foote, J., Neuberger, M. S. & Winter, G. Replacing the complementarity-determining regions in a human antibody with those from a mouse. *Nature* **321**, 522–525 (1986).
22. Li, H.-S. *et al.* Multidimensional control of therapeutic human cell function with synthetic gene circuits. *Science* **378**, 1227–1234 (2022).
23. Rauch, S. *et al.* Programmable RNA-Guided RNA Effector Proteins Built from Human Parts. *Cell* **178**, 122-134.e12 (2019).
24. Zhu, I. *et al.* Design and modular assembly of synthetic intramembrane proteolysis receptors for custom gene regulation in therapeutic cells. *BioRxiv* (2021) doi:10.1101/2021.05.21.445218.
25. Danser, A. H. J. & Deinum, J. Renin, prorenin and the putative (pro)renin receptor. *Hypertension* **46**, 1069–1076 (2005).
26. Vaidyanathan, S., Jarugula, V., Dieterich, H. A., Howard, D. & Dole, W. P. Clinical pharmacokinetics and pharmacodynamics of aliskiren. *Clin. Pharmacokinet.* **47**, 515–531 (2008).
27. Puskas, J. *et al.* Development of an attenuated interleukin-2 fusion protein that can be activated by tumour-expressed proteases. *Immunology* **133**, 206–220 (2011).
28. Hsu, E. J. *et al.* A cytokine receptor-masked IL2 prodrug selectively activates tumor-infiltrating lymphocytes for potent antitumor therapy. *Nat. Commun.* **12**, 2768 (2021).
29. Wang, X., Wong, K., Ouyang, W. & Rutz, S. Targeting IL-10 Family Cytokines for the Treatment of Human Diseases. *Cold Spring Harb. Perspect. Biol.* **11**, (2019).
30. Sarvas, J. L., Khaper, N. & Lees, S. J. The IL-6 Paradox: Context Dependent Interplay of SOCS3 and AMPK. *J. Diabetes Metab.* **Suppl 13**, (2013).
31. Serrano, A. L., Baeza-Raja, B., Perdiguero, E., Jardí, M. & Muñoz-Cánoves, P. Interleukin-6 is an essential regulator of satellite cell-mediated skeletal muscle hypertrophy. *Cell Metab.* **7**, 33–44 (2008).
32. Zhang, C. *et al.* Interleukin-6/signal transducer and activator of transcription 3 (STAT3) pathway is essential for macrophage infiltration and myoblast proliferation during muscle regeneration. *J. Biol. Chem.* **288**, 1489–1499 (2013).
33. Liao, W., Lin, J.-X. & Leonard, W. J. Interleukin-2 at the crossroads of effector responses, tolerance, and immunotherapy. *Immunity* **38**, 13–25 (2013).
34. Rosenberg, S. A. Interleukin 2 for patients with renal cancer. *Nat. Clin. Pract. Oncol.* **4**, 497 (2007).
35. Hawkins, E. R., D'Souza, R. R. & Klampatsa, A. Armored CAR T-Cells: The Next Chapter in T-Cell Cancer Immunotherapy. *Biologics* **15**, 95–105 (2021).

485 36. Logsdon, N. J., Jones, B. C., Josephson, K., Cook, J. & Walter, M. R. Comparison of
486 interleukin-22 and interleukin-10 soluble receptor complexes. *J. Interferon Cytokine Res.*
487 **22**, 1099–1112 (2002).
488 37. Gorby, C. *et al.* Engineered IL-10 variants elicit potent immunomodulatory effects at low
489 ligand doses. *Sci. Signal.* **13**, (2020).
490 38. Garbers, C. *et al.* Plasticity and cross-talk of interleukin 6-type cytokines. *Cytokine*
491 *Growth Factor Rev.* **23**, 85–97 (2012).
492 39. Wolf, J., Rose-John, S. & Garbers, C. Interleukin-6 and its receptors: a highly regulated
493 and dynamic system. *Cytokine* **70**, 11–20 (2014).
494 40. Kwon, B. The two faces of IL-2: a key driver of CD8+ T-cell exhaustion. *Cell. Mol.*
495 *Immunol.* **18**, 1641–1643 (2021).
496 41. Shikano, S. & Li, M. Membrane receptor trafficking: evidence of proximal and distal
497 zones conferred by two independent endoplasmic reticulum localization signals. *Proc*
498 *Natl Acad Sci USA* **100**, 5783–5788 (2003).
499 42. Fukamizu, A. *et al.* Dependence of angiotensin production in transgenic mice carrying
500 either the human renin or human angiotensinogen genes on species-specific kinetics of
501 the renin-angiotensin system. *Arzneimittelforschung* **43**, 222–225 (1993).
502 43. Wu, Z., Yang, H. & Colosi, P. Effect of genome size on AAV vector packaging. *Mol.*
503 *Ther.* **18**, 80–86 (2010).
504 44. Kalidasan, V. *et al.* A guide in lentiviral vector production for hard-to-transfect cells,
505 using cardiac-derived c-kit expressing cells as a model system. *Sci. Rep.* **11**, 19265
506 (2021).
507 45. Tang, W. *et al.* Faithful expression of multiple proteins via 2A-peptide self-processing: a
508 versatile and reliable method for manipulating brain circuits. *J. Neurosci.* **29**, 8621–8629
509 (2009).
510 46. Subramanian, N., Torabi-Parizi, P., Gottschalk, R. A., Germain, R. N. & Dutta, B.
511 Network representations of immune system complexity. *Wiley Interdiscip. Rev. Syst. Biol.*
512 *Med.* **7**, 13–38 (2015).
513 47. Orzechowski, A. Cytokines in skeletal muscle growth and decay. in *The plasticity of*
514 *skeletal muscle* (ed. Sakuma, K.) 113–139 (Springer Singapore, 2017). doi:10.1007/978-
515 981-10-3292-9_5.
516 48. Yang, W. & Hu, P. Skeletal muscle regeneration is modulated by inflammation. *J.*
517 *Orthop. Translat.* **13**, 25–32 (2018).
518 49. Steyn, P. J., Dzobo, K., Smith, R. I. & Myburgh, K. H. Interleukin-6 Induces Myogenic
519 Differentiation via JAK2-STAT3 Signaling in Mouse C2C12 Myoblast Cell Line and
520 Primary Human Myoblasts. *Int. J. Mol. Sci.* **20**, (2019).
521 50. Deng, B., Wehling-Henricks, M., Villalta, S. A., Wang, Y. & Tidball, J. G. IL-10 triggers
522 changes in macrophage phenotype that promote muscle growth and regeneration. *J.*
523 *Immunol.* **189**, 3669–3680 (2012).
524 51. Coppola, C. *et al.* Investigation of the Impact from IL-2, IL-7, and IL-15 on the Growth
525 and Signaling of Activated CD4+ T Cells. *Int. J. Mol. Sci.* **21**, (2020).
526 52. Nielsen, M. & Andreatta, M. NetMHCpan-3.0; improved prediction of binding to MHC
527 class I molecules integrating information from multiple receptor and peptide length
528 datasets. *Genome Med.* **8**, 33 (2016).
529 53. Calis, J. J. A. *et al.* Properties of MHC class I presented peptides that enhance
530 immunogenicity. *PLoS Comput. Biol.* **9**, e1003266 (2013).

54. Vaidyanathan, S. *et al.* Pharmacokinetics, safety, and tolerability of the novel oral direct renin inhibitor aliskiren in elderly healthy subjects. *J. Clin. Pharmacol.* **47**, 453–460 (2007).
55. Gradman, A. H. *et al.* Aliskiren, a novel orally effective renin inhibitor, provides dose-dependent antihypertensive efficacy and placebo-like tolerability in hypertensive patients. *Circulation* **111**, 1012–1018 (2005).
56. Kishina, M. *et al.* Therapeutic effects of the direct renin inhibitor, aliskiren, on non-alcoholic steatohepatitis in fatty liver Shionogi ob/ob male mice. *Hepatol. Res.* **44**, 888–896 (2014).

Methods

Plasmid generation. All plasmids were constructed using general practices. Backbones were linearized via restriction digestion, and inserts were generated using PCR, phosphorylated annealing, or purchased from Twist Biosciences. A complete list of plasmids used for each experiment (Supplementary Data 1) and the respective amounts used for transfection can be found in Supplementary Data 2. In addition, the DNA sequences of all the plasmids used in this study can be found in the source data, and all new plasmids with annotations will be available on Addgene.

mRNA synthesis. The DNA templates for in vitro transcription were prepared by PCR on a plasmid template containing hDIRECT coding sequences flanked by optimal 5' and 3' UTRs as well as a T7 promoter. The plasmid template with optimal UTRs was a gift from Prof. Michael Elowitz. Poly-A tail was added to the DNA template by PCR using Q5 PCR master mix (New England Biosciences, M0494L) with reverse primer containing a 200 bp polyA sequence. PCR products were cleaned and concentrated using DNA Clean & Concentrator kit (Zymo Research, D4033).

In vitro transcript mRNA was synthesized from DNA template using HiScribe IVT kit (New England Biosciences, E2040S) and using 100% N1-methyl-psuedouridine-5'-triphosphate modified (Trilink, N-1081-10) bases to improve RNA expression and with murine RNase inhibitor to improve RNA yield (New England Biosciences, M0314). mRNA was co-transcriptionally capped with a Cap 1 structure using CleanCapAG (Trilink, N-7113). Synthesized RNA was purified using Monarch RNA Cleanup kit (New England Biosciences, T2040).

Tissue culture. WT Human Embryonic Kidney (HEK) 293 cells (ATCC, catalog no. CRL-1573) and HEK293T-LentiX (Takara Biosciences, catalog no. 632180), were cultured in a humidity-controlled incubator under standard culture conditions (37 °C with 5% CO_2) in Dulbecco's modified Eagle's medium (DMEM), supplemented with 10% fetal bovine serum (Fisher Scientific, catalog no. FB12999102), 1 mM sodium pyruvate (EMD Millipore, catalog no. TMS-005-C), 1× penicillin–streptomycin (Genesee, catalog no. 25-512), 2 mM l-glutamine (Genesee, catalog no. 25-509) and 1× MEM non-essential amino acids (Genesee, catalog no. 25-536). HEKBlue™ IL-2, IL-6, and IL-10 cells were purchased from Invivogen (catalog no. hkb-il2, hkb-hil6, hkb-il10, respectively). Cells were cultured as per manufacturer's protocol. T-REx™ Jurkat cells (Invitrogen, catalog no. R72207) and WT K-562 cells (gift from the Prof. Lacramioara Bintu, ATCC, catalog no. CCL-243) were cultured in a humidity-controlled

incubator under standard culture conditions (37 °C with 5% CO_2) in RPMI 1640 (Gibco, catalog no.11875093, supplemented with 10% heat-inactivated fetal bovine serum (Fisher Scientific, catalog no. FB12999102) and 1× penicillin–streptomycin (Genesee, catalog no. 25-512).

Transient transfection. Plasmid DNA. HEK293 cells were cultured in 96-well tissue culture-treated plates under standard culture conditions. When cells were 70-90% confluent, the cells were transiently transfected with plasmid constructs using the jetOPTIMUS DNA transfection reagent (Polyplus, catalog no. 117-15), as per manufacturer's instructions using 0.375 μL of reagent per 50 μL of jetOPTIMUS buffer for 500 ng total DNA transfections. Experiments requiring incubation with aliskiren (Sigma Aldrich, catalog no. SML2077) were treated with drug at time of transfection through media exchange. Drug was titrated from 0.5-500,000 nM of aliskiren in 10x increments.

mRNA. HEK293 cells were cultured in 24-well tissue culture-treated plates under standard culture conditions. When cells were 70-90% confluent, the cells were transiently transfected with mRNA using the Lipofectamine™ MessengerMAX mRNA Transfection Reagent (Invitrogen, LMRNA001), as per manufacturer's instructions using 1 μL reagent per 50 μL reaction/well for a 500 ng total mRNA transfection. Experiments requiring incubation with aliskiren were treated with drug at time of transfection through media exchange. Drug was titrated from 0.5-500,000 nM of Aliskiren in 10x increments.

Lentiviral transduction. LentiX cells were cultured in 6-well tissue culture-treated plates under standard culture conditions. When cells were 70-90% confluent, the cells were transiently transfected with plasmid constructs (600 ng PAX2, pMD2g, and 1,100 ng transfer target) using the jetOPTIMUS DNA transfection reagent (Polyplus catalog no. 117-15), as per manufacturer's instructions using 1.5 μL of reagent per 200 μL of jetOPTIMUS buffer for 2,000 ng total DNA transfections. Cells were incubated for 24 h under standard culture conditions. Afterwards an additional 3 mL of DMEM media was added carefully to each well. Lentivirus was concentrated 24 hrs afterward using viral precipitation. For each lentiviral prep, media was filtered using a syringe and 0.45 μm filter into 15 mL conical tubes. 5x Lentivirus Precipitation Solution (Alstem catalog no. VC100) was mixed with each prep and incubated at 4 °C overnight. Then, virus was spun down at 1500xg for 30 min at 4 °C. Supernatant was aspirated, and virus was resuspended using 200 μL Dulbecco's PBS (Genesee catalog no. 25-508). Virus was added dropwise onto 24-well tissue culture plates containing HEK293, K-562, or Jurkat cells seeded at 250k cells/well. 72 h after incubation, the percentage of mCherry-positive cells were quantified using flow cytometry. The cells were selected using 1000 ng/mL of puromycin (ThermoFisher Scientific; catalog# J61278-MB) for one week until >90% of cells were mCherry-positive before being used for experiments.

Cytokine reporter cell assay. Supernatant (10 μL) from HEK293 cells transiently transfected 24 h prior were incubated with 53,200 HEKBlue™ cells (190 μL) in 96-well tissue culture-treated plates for 24 h under standard culture conditions. Afterwards, 20 μL HEKBlue™ cell supernatant was collected and incubated with 180 μL Quanti-Blue reagent (Invivogen) for 2 h at 37 C as per manufacturer protocol. The mixture was read at 630 nm using the Spark® Multimode microplate reader (TECAN). Cartoon schematic can be found in Supplementary Fig. 1.

623 For stable transductions, stable HEK293 cells were seeded at 7,500 cells (unless otherwise
624 specified) in 96-well tissue culture-treated plates for 48 h under standard culture conditions.
625 Media was changed either with or without aliskiren 24 h into the incubation. Supernatant transfer
626 to HEKBlue™ cells and assay proceeded the same as prior. Jurkat cells were seeded at 50,000
627 cells in U-bottom 96-well plates for 48 h under standard culture conditions. Cells were spun
628 down in a centrifuge at 300 xg for 7 min and media was replaced with or without aliskiren 24 h
629 into the incubation. 48 h after seeding, cells were spun down in a centrifuge at 300 xg for 7 min
630 again and supernatant was transferred to HEKBlue™ cells and assay proceeded the same as
631 prior.
632
633 **Western blot.** HEK293 cells in 24-well tissue culture-treated plates were transiently transfected
634 using transfection protocols mentioned prior. 24 hours after transient transfection, media was
635 exchanged with serum-free, supplemented DMEM at half the volume (250 uL). Conditions
636 requiring incubation with Aliskiren were treated with drug during media exchange. 48 hours
637 after transient transfection, 16 μL of supernatant was incubated with 20 μL Tris-Glycine SDS
638 sample buffer (2X) (ThermoFisher LC2676) and 4 μL NuPage Sample Reducing Agent (10X)
639 (ThermoFisher NP0009) at 85 °C for 3 min. Samples and 5 μL PageRuler Prestained Protein
640 Ladder (ThermoFisher 26616) were loaded onto 10-well Novex Tris-Glycine mini gels (16%)
641 (ThermoFisher XP00160BOX).
642
643 Gels were transferred using a Mini Blot Module (ThermoFisher B1000) and a PVDF/Filter paper
644 membrane sandwich (ThermoFisher LC2002). Sponges were soaked in 1x Tris-Glycine Transfer
645 Buffer (ThermoFisher LC3675) and the PVDF membrane was activated by submerging in 100%
646 ethanol prior to stacking. After blotting, the membrane was blocked using 5% nonfat dry milk
647 (Apex catalog no. 20-241) in 1x DPBS (Genesee catalog no. 25-508) for 1 hour at room
648 temperature with shaking. After blocking, the membrane was incubated with a primary Rb anti-
649 myc antibody (Abcam, catalog AB9106) at a 1/2500 dilution in a 1% bovine serum albumin
650 (BSA) (UniRegion, UR-BSA001-100G) solution with DPBS overnight at 4 °C with shaking.
651 The following day, the membrane was washed in 1x DPBS with 0.1% Polysorbate 20
652 (ThermoScientific, catalog J66278.AE) for 15 min at room temperature with shaking. The wash
653 was repeated three more times, 5 minutes each, with shaking at room temperature. After the final
654 wash, the membrane was incubated with a secondary anti-Rb IgG antibody (Abcam, AB205718)
655 (1/1000 dilution) in a 1% BSA solution with DPBS for 1 hour at room temperature with shaking.
656 After incubation, the membrane was washed again for 3 additional times, 5 minutes each, at
657 room temperature with shaking. The membrane was incubated with an ECL substrate kit
658 (Abcam, AB133406) for 2 minutes prior to imaging on an iBright CL1500 imager (Invitrogen)
659 using the ChemiBlot protocol.
660
661 **Kinetic experiments.** Induction. Stable HEK293 cells expressing the single transcript construct
662 were split at 15,000 cells/well in a tissue-culture treated 96-well plate. 24 hours later, media was
663 exchanged with fresh media or media containing 5,000 nM aliskiren. 10 μL supernatant was
664 transferred from individual biological replicates at varying timepoints (30 min to 24 hrs) to
665 another 96-well plate which was stored at 4 °C to preserve the samples. After the final
666 supernatant collection, 50,000 HEKBlue™ IL-10 cells/well (190 μL) was transferred to the 96-
667 well plates containing the supernatant samples and incubated for 24 h under standard culture
668 conditions. Afterwards, 20 μL HEKBlue™ IL-10 cell supernatant was collected and incubated

669 with 180 µL Quanti-Blue reagent (Invivogen) for 2 h at 37 C as per manufacturer protocol. The
670 mixture was read at 630 nm using the Spark® Multimode microplate reader (TECAN).
671
672 Reversibility. Cells were prepared in the same manner as the "Induction" section. 2 hours after
673 seeding, media was exchanged with fresh media or media containing 5,000 nM aliskiren. 24
674 hours later, drug was removed from all conditions with a fresh media change. Supernatant was
675 transferred, stored, and assayed in the same manner as the "Induction" section.
676
677 **HEKBlue reporter cell recombinant cytokine titration.** Fresh serial dilutions of recombinant
678 human IL-2 (PeproTech, AF-200-02), IL-6 (PeproTech, 200-06), and IL-10 (PeproTech, 200-10)
679 were prepared with PBS. 10 µL samples at each concentration were incubated with 50,000
680 HEKBlue™ cells (190 µL) in 96-well tissue culture-treated plates for 24 h under standard culture
681 conditions. HEKBlue™ cell supernatant was assayed for reporter cell activity as previously
682 mentioned in "cytokine reporter cell assay" above.
683 HEKBlue™ IL-2 activity standard curve was obtained using a three-parameter nonlinear fit with
684 GraphPad Prism 10 to relate OD (630 nM) measurements to cytokine concentration (ng/mL).

685 $$Y = Bottom + X * \frac{Top - Bottom}{EC50 + X}$$

686 Or

687 $$X = EC50 * \frac{Y - Bottom}{Top - Y}$$

688 Where Y = OD (630 nM) and X = [Cytokine concentration] (ng/mL).
689
690 **Flow cytometry.** Flow Cytometry was performed on ZE5 Cell analyzer (BioRad). Samples were
691 prepared in 50 µL culture media and diluted 1:1 with Hank's Balanced Salt Solution (Cytiva,
692 SH30588.01) + 0.25% BSA and measured in biological triplicate. Live cells were gated via
693 forward (FSC) and side (SSC) scatter. For mCherry-expressing cells, fluorescence was measured
694 using 561nm excitation laser with a 615/24 nm emission filter. Flow cytometry data was
695 analyzed using FlowJo (BD). T cells were gated from engineered K-562 cells by gating on the
696 presence of mCherry and total cell counts for mCherry$^-$ cells were determined. Flow cytometry
697 data was further processed using Prism 9 software (GraphPad).
698
699 **Fluorescence activated cell sorting (FACS).** To sort K-562 cells stably integrated with
700 hDIRECT-IL2 cassettes, samples were concentrated to $5x10^6$ cells/mL in 250 uL. Lives cells
701 were gated by forward scatter (FSC) and side scatters (SSC). Fluorescence data was collected for
702 mCherry (excitation laser: 561nm) Gated populations of cells expressing mCherry were sorted
703 on a FACSAria II (BD Biosciences) into fresh RPMI 1640 + 10% heat inactivated FBS + 1 %
704 penicillin–streptomycin. K-562 cells were cultured for 3 days and allowed to reach confluency of
705 $1x10^6$ cells/mL before staring co-culture experiments.
706
707 **Human primary T cell culture.** Primary T cells were isolated from a peripheral blood
708 mononuclear cells (PBMCs) Leuko Pak from a healthy donor (StemCell, catalog no. 70500.1) by
709 using the EasySep Human T Cell Isolation kit (STEMCELL, catalog no. 17951). Cells were
710 frozen down using Cellbanker 1 (AimsBio, 11910). Cells were cultured in X-Vivo15 medium,
711 (Lonza, catalog no. 04418Q) supplemented with 1 mM N-Acetyl-L-cysteine (Thermo scientific,
712 A15409.22), 55 uM 2-Mercaptoethanol (Gibco, 21985-023), 5% heat inactivated human AB

713 serum (BioIVT, HP1022HI), pH balanced with 1N NaOH (Fisher Scientific, SS255-1), and 200
714 U/mL IL-2 (Fredrick National Lab BRB Preclinical Repository).
715
716 **In vitro T cell proliferation co-culture.** T cells were thawed and plated in 24-well plates at a
717 density of $1x10^6$ cells/mL. T cells were activating using CD3/CD28 Human T-Activator
718 Dynabeads (Gibco, 11131D) at a 3:1 bead:cell ratio for 48 hours. Beads were removed via
719 magnetic separation, and cells were cultured for 48 hours prior to proliferation assay.
720 T cells were counted using Denovix CellDrop automated cell counter and plated in a 96-well
721 untreated round-bottom plate at 25,000 cells/well in 50 µL media. T cells were co-cultured with
722 25,000 cells of either sorted, hDIRECT engineered K-562 cells or wild-type K-562 cells, both
723 engineered to express mCherry. Cell culture was brought up to 100 uL X-Vivo 15 media per
724 well. Populations were treated with either 5000 nM Aliksiren, vehicle control, or 200 U/mL IL-2.
725
726 T cell counts were analyzed using flow cytometry to count live cells by gating on FSC/SSC and
727 mCherry. Cells were prepared for flow cytometry on days 0, 2, 4, and 6 by removing 50 uL of
728 well-dispersed cell culture and diluting 1:1 in HBSS + 0.25% BSA. On day 3, cells were
729 centrifuged at 100xg for 10 minutes and media was replaced. Spent media was analyzed for IL-2
730 concentration via ELISA.
731
732 **Human IL-2 ELISA.** ELISA was performed with 50 µL of supernatant from cultured T cells
733 using Human IL-2 ELISA (Abcam, ab270883) according to manufactures instructions.
734 Absorbance was measured at 450 nm using Tecan Infinite M Plex microplate reader. All ELISA
735 measurements were performed in biological triplicates. Samples with absorbance higher than
736 standard ladders provided were diluted until within range of the provided standards. IL-2
737 concentrations were calculated via interpolation of a four-parameter curve fit, and diluted
738 samples were adjusted via linear scaling in accordance with the manufacturer recommendation.
739
740 **In vivo control of human renin via aliskiren.**
741 Animal studies were conducted at Stanford University with the approval of the Stanford
742 Administrative Panel on Laboratory Animal Care (#34743). Female BALB/c mice 12-14 weeks
743 of age were randomly assigned to each experimental group. Aliskiren hemifumarate
744 (MedChemExpress, HY-12177) was prepared at 20 mg/mL in PBS pH 7.4 (Gibco, 10010023)
745 and given at a dose of 100 mg/kg p.o. 2 hours prior to plasmid delivery via 1 mL syringe with a
746 20G 1.5" feeding tube (BrainTree, DT9920). Following initial drug dosing, plasmids were
747 delivered via hydrodynamic gene delivery. All mice received plasmid delivery of 8 µg of
748 membrane-bound, renin cleavable NanoLuciferase and 4 µg of CMV-driven secreted embryonic
749 alkaline phosphatase (SEAP) as a co-secretion marker. Treatment groups received an additional
750 4 ug of CMV-driven human renin plasmid. Plasmids were diluted in 2 mL Trans-IT EE delivery
751 solution (Mirus, MIR 5340) were delivery intravenously via tail vein using 5 mL syringes with a
752 27G needle (Air-Tite, N2712) in less than 10 seconds. Aliskiren dosing was repeated at 100
753 mg/kg 2 hours following plasmid delivery. 4 hours following final aliskiren administration,
754 blood samples were collected via saphenous vein puncture into a clotting capillary tube for
755 serum collection. High doses of aliskiren were given to mice due to the low bioavailability of
756 aliskiren in mice relative to humans[56]. Samples were centrifuged at 2000xg for 10 minutes to
757 isolate serum. Serum levels of cleaved NanoLuciferase were measured by diluting 5 µg of serum
758 in 45 µL of DI water and NanoLuciferase was measured using NanoGlo Luciferase Assay

759 system (Promega, N1120). Luminescence was measured using Infinite M Plex microplate reader
760 (TECAN) with a 1000 ms integration time. Serum luciferase levels were normalized to SEAP
761 serum values measured using Phospha-Light SEAP Reporter Gene Assay system (Applied
762 Biosciences, T1015) by diluting 5 µL serum in 45 µL of the provided diluent.
763 Chemiluminescence was measured using Infinite M Plex microplate reader (TECAN) with a 100
764 ms integration time.
765
766 **Bioinformatic Analysis of Predicted MHC-I Binding and Immunogenicity.** Immunogenicity
767 of viral proteases was compared to engineered human proteases using the Immune Epitope
768 Database & Tools (IEDB) platform (https://www.iedb.org/). Peptide sequences were obtained
769 from literature for TEVp and HCVp and directly compared with the sequence from ER-H2M-
770 Renin, the most engineered human protease reported here. The sequence for each peptide was
771 sequentially tiled into peptides of length 9, and a Protein BLAST using NCBI blastp
772 (https://blast.ncbi.nlm.nih.gov/Blast.cgi) was performed on each 9-mer peptide to search for
773 exact sequence matches to human proteins in the Protein Data Bank. Any exact matches to
774 human protein sequences were excluded from further analysis, as these peptides were assumed to
775 be non-immunogenic and therefore a source of potential false positives. Nonhuman 9-mer
776 peptide sequences were then analyzed using IEDB's MHC I Binding Affinity predictor
777 (NetMHCpan4.1 BA), where peptides with binding affinities less than or equal to 500 nM are
778 considered likely to bind to and be presented by MHC I complexes[52]. HLA-A*02:01 was
779 selected for our analysis since it is the most commonly analyzed HLA allele. The MHC I
780 Immunogenicity predictor was also used with default settings to get predictions of how likely
781 each pMHC complex would be to elicit an immune response.
782
783 **IFN-γ ELISPOT.** H2M-renin peptide immunogenicity was assayed using a human IFN-γ single-
784 color enzymatic ELISPOT assay kit (CTL, hIFNg-1M/2) according to the manufacturer's
785 recommendation. A custom synthesized H2M-renin peptide pool was purchased from Elim
786 Biopharm (28 9-mer peptides, 1mg/peptide). Peptide pool was initially reconstituted to 1 mg/mL
787 in sterile PBS. Frozen vials of PBMCs from four healthy donors (HLA-A*02:01) were purchased
788 from (StemCell, catalog no. 70107). 96-well plates were coated with a human IFN-γ capture
789 solution and sealed overnight with parafilm at 4 C.
790
791 The next day, donor PBMCs were rapidly thawed in a 37C water bath and washed with RPMI
792 1640 + 1% L-glutamine (Genesee, catalog no. 25-509) prior to 10 minutes of centrifugation at
793 330 xg. Cells were counted using Denovix CellDrop automated cell counter and resuspended in
794 CTL-Test medium (CTL, CTL-010) to $3x10^6$ cells/mL. 2x antigen solutions of the peptide pool
795 were prepared at 0.2, 2, 20 µg/mL using CTL-Test media. CERI-MHC Class I Control Peptide
796 Pool (CTL, CTL-CERI-300) was diluted 1:20 using CTL-Test media. The coated plates were
797 decanted and washed with sterile PBS. Antigen (H2M-renin peptide pool dilutions), positive
798 control (CERI dilution), and negative control (CTL-Test medium) were plated at 100 µL/well in
799 triplicates and incubated for 10 minutes in a 37 C incubator. PBMCs were plated at 100 µL/well
800 (300k cells/well) onto sample wells and incubated for 24 hours at 37 C.
801 The next day, plates were washed a total of three times with sterile PBS and 0.05% Tween-PBS
802 prior to incubating with 80 µL/well of anti-human IFN-γ detection solution for 2 hours at room
803 temperature. Plates were washed three times again with 0.05% Tween-PBS prior to incubating
804 with 80 µL/well of a Tertiary Solution for 30 minutes at room temperature. Plates were washed

with 0.05% Tween-PBS twice, followed by two washes with distilled water. Plates were incubated with 80 μL/well of Blue Developer Solution for 15 minutes at room temperature and the reaction was stopping by rinsing the membrane with tap water three times. Plates were air-dried overnight at room temperature, avoiding exposure to light. The plates were sent to Cellular Technology Limited (CTL) for scanning and analysis of spot forming units (SFU). Wells unable to be precisely quantified due to overly numerous spot formations are labeled too numerous to count (TNTC).

Statistical analysis. For experiments comparing two groups, an unpaired two-tailed Student's *t*-test was used to assess significance. Single, double, triple, and quadruple asterisks indicate $P < 0.05$, $P < 0.01$, $P < 0.001$ and $P < 0.0001$ unless corrected for multiple comparisons using a Bonferroni correction. EC50 and IC50 measurements for curves were calculated using GraphPad Prism and reported as mean +- standard error of the mean (s.e.m.). A one-way ANOVA was used to compare the means among different experiment groups. All statistical analyses were performed using GraphPad Prism 10.0.0.

Data availability.

All data reported in this paper are available from the corresponding author on request. Plasmid maps for all plasmids used in this study will be available as GenBank files. The plasmids used in this study will be deposited on Addgene, with complete and annotated GenBank files on their website. All figures and supplemental figures have associated raw data. There are no restrictions on data availability.

Acknowledgements.

This research was supported by NIH (R00EB027723, DP2OD034951; X.J.G), Longevity Impetus Grants (X.J.G.), Wu Tsai Human Performance Alliance Agility Project Grant (X.J.G.), Stanford Bio-X Interdisciplinary Initiatives Seed Grant Program (IIP) [R11-7] (X.J.G.), the Stanford Graduate Fellowship (C.A.), the Sarafan ChEM-H CBI training program (C.A.), the Bio-X Stanford Interdisciplinary Graduate Fellowship (C.A.), the CMB training grant NIH (T32 GM007276; C.C.C.), the National Science Foundation Graduate Research Fellowship (DGE-2146755; C.C.C.), and the International Human Frontier Science Program Organization (LT000221/2021-L; A.E.V.).

Author contributions.

C.A.A. and X.J.G. conceived and directed the study. C.A.A. designed and performed all experiments for the protein engineering and characterization. C.C.C. designed and performed the T cell proliferation and in vivo study. A.E.V. created the transmembrane domain and ER-retention motifs for renin constructs, as well as performed tail vein injections for the in vivo study. J.P. and Q.C. provided recommended mutations for the H2M renin. L.E.S. conducted the computational immunogenicity analysis. C.A.A. and C.C.C. analyzed the data for the manuscript. C.A.A., X.J.G., and C.C.C. wrote the manuscript. All authors provided feedback on the manuscript.

Competing interests.

The board of trustees of the Leland Stanford Junior University have filed a patent on behalf of the inventors (C.A.A. and X.J.G.) of the small-molecule control of membrane and secreted

proteins using human proteases platform described (US provisional Application No. 63/458833). An additional provisional patent application has also been filed on behalf of the inventors (C.A.A., X.J.G., J.P, and Q.C.) for the orthogonalization of human renin. X.J.G. is a co-founder and serves on the scientific advisory board of Radar Tx.

856 **Figures:**

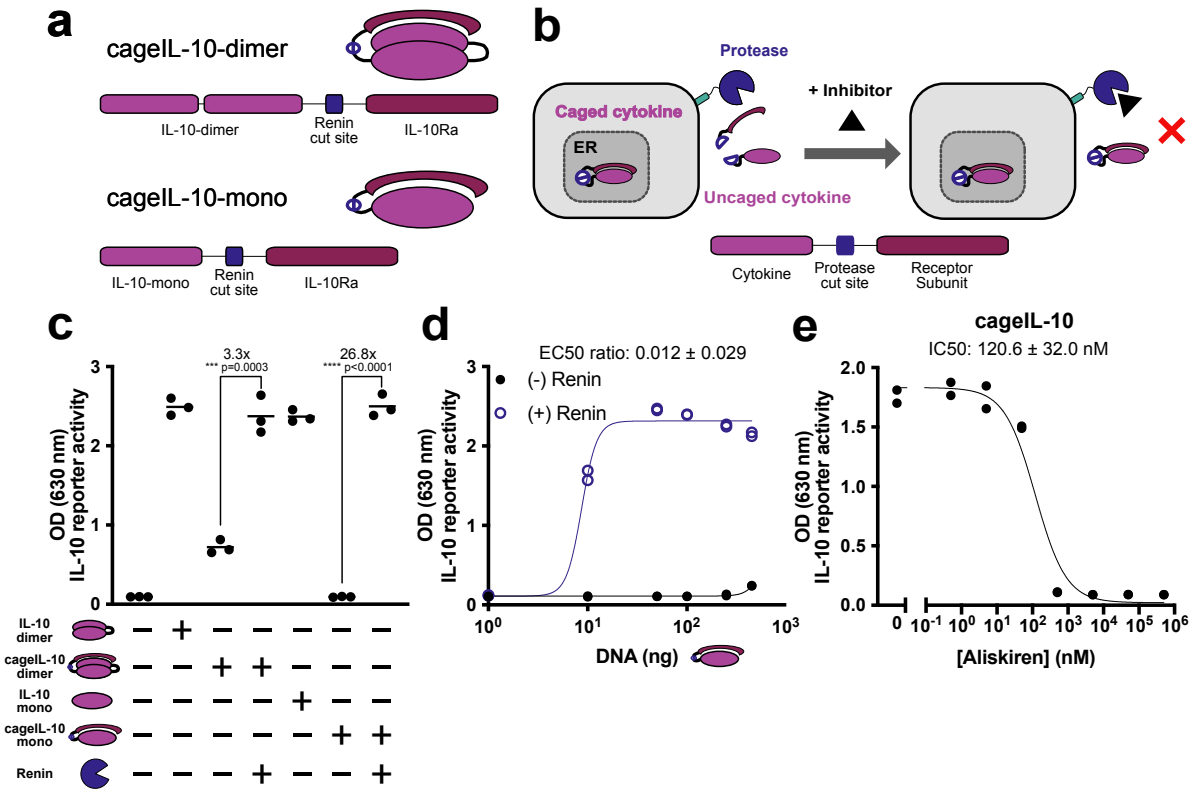

Fig. 1: Engineering caged IL-10. a, Caged cytokine design for dimeric and monomeric IL-10. Cytokines are fused with renin-cleavable linkers to cognate receptor subunits, inhibiting binding to cellular receptors. **b,** hDIRECT circuit using caged cytokines to control cytokine activity. Cells constitutively secrete attenuated caged cytokines and cytokine activity can be tuned down via small-molecule inhibitor for co-transfected protease, renin. **c,** Functional activity of caged IL-10 constructs with or without renin co-expression. **d,** Functional activity of cageIL-10 plasmid transiently transfected with increasing amounts, with or without renin co-expression. **e,** Functional activity of cageIL-10 co-expressed with renin at increasing aliskiren concentrations. (For **c-e**: Cytokine activity measured from supernatant using HEKBlue IL-10™ reporter cells. For **c**: mean of n = 3 biological replicates; Unpaired two-tailed Student's t-test. For **d-e**: n = 2 biological replicates; data represent mean ± s.e.m. *** $p \leq 0.001$, **** $p < 0.0001$.)

857
858

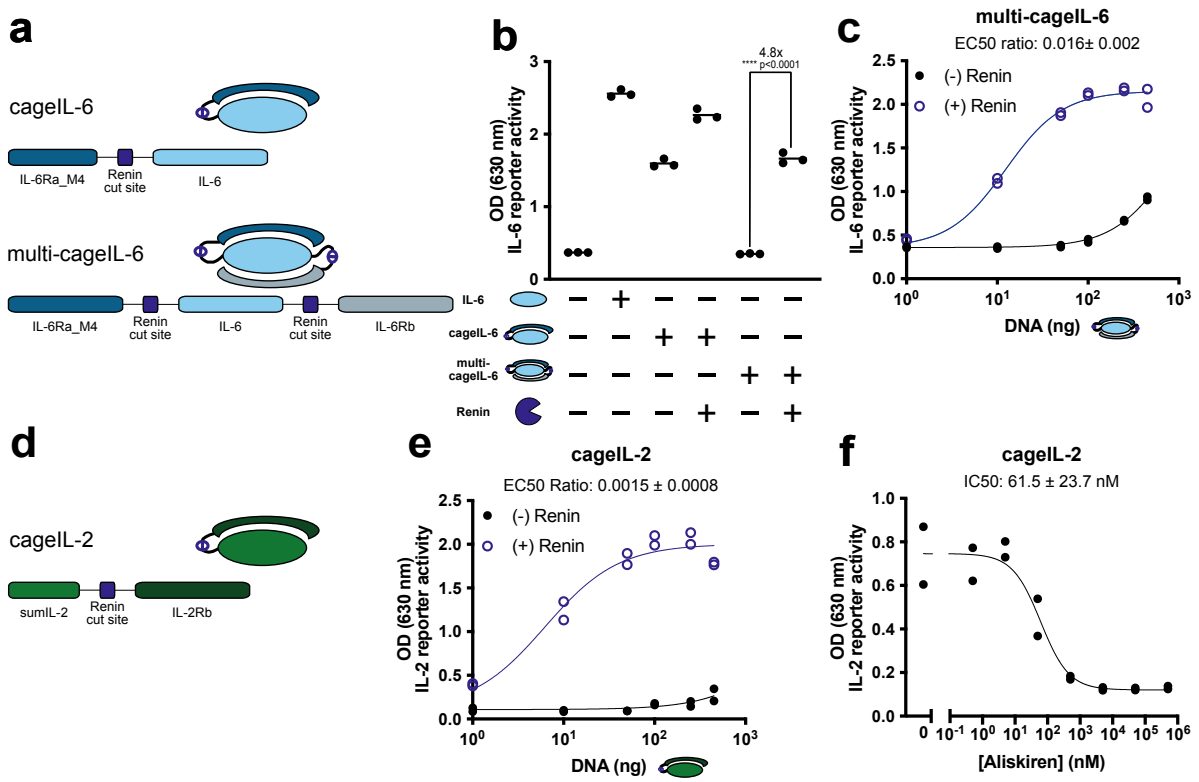

Fig. 2: Engineering caged IL-6 and IL-2. a, Caged cytokine design for single and multi-caged IL-6 constructs. **b,** Functional activity of caged IL-6 constructs with or without renin co-expression. **c,** Functional activity of multi-cageIL-6 plasmid transiently transfected with increasing amounts, with or without renin co-expression. **d,** Caged cytokine design for caged IL-2. **e,** Functional activity of cageIL-2 plasmid transiently transfected with increasing amounts, with or without renin co-expression. **f,** Functional activity of cageIL-2 co-expressed with renin at increasing aliskiren concentrations. (Cytokine activity measured from supernatant using HEKBlue IL-6™ (**b-c**) and IL-2™ (**e-f**) reporter cells. For **b**: mean of n = 3 biological replicates; Unpaired two-tailed Student's t-test. For **c,e-f**: n = 2 biological replicates; data represent mean ± s.e.m. **** $p < 0.0001$.)

859
860

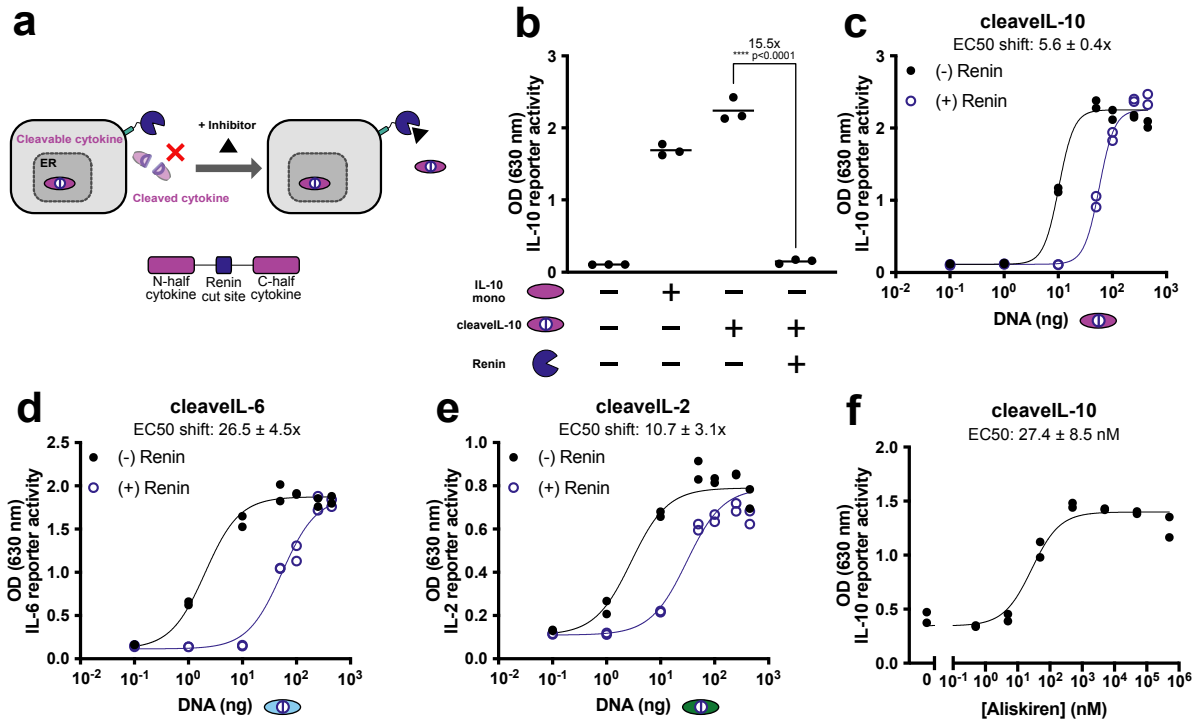

Fig. 3: Engineering of cleavable cytokines. a, hDIRECT circuit using cleavable cytokines to control cytokine activity. Cells constitutively secrete cleavable cytokines and cytokine activity can be tuned via small-molecule inhibitor for co-transfected protease, renin. **b,** Functional activity of cleaveIL-10 with or without renin co-expression. **c,** Functional activity of cleaveIL-10 plasmid transiently transfected with increasing amounts, with or without renin co-expression. **d,** Functional activity of cleaveIL-6 plasmid transiently transfected with increasing amounts, with or without renin co-expression. **e,** Functional activity of cleaveIL-2 plasmid transiently transfected with increasing amounts, with or without renin co-expression. **f,** Functional activity of cleaveIL-10 co-expressed with renin at increasing aliskiren concentrations. (Cytokine activity measured from supernatant using HEKBlue IL-10™ (**b-c,f**), IL-6™ (**d**), and IL-2™ (**e**) reporter cells. For **b**: mean of n = 3 biological replicates; Unpaired two-tailed Student's t-test. For **c-f**: n = 2 biological replicates; data represent mean ± s.e.m. **** $p < 0.0001$.)

861
862
863
864

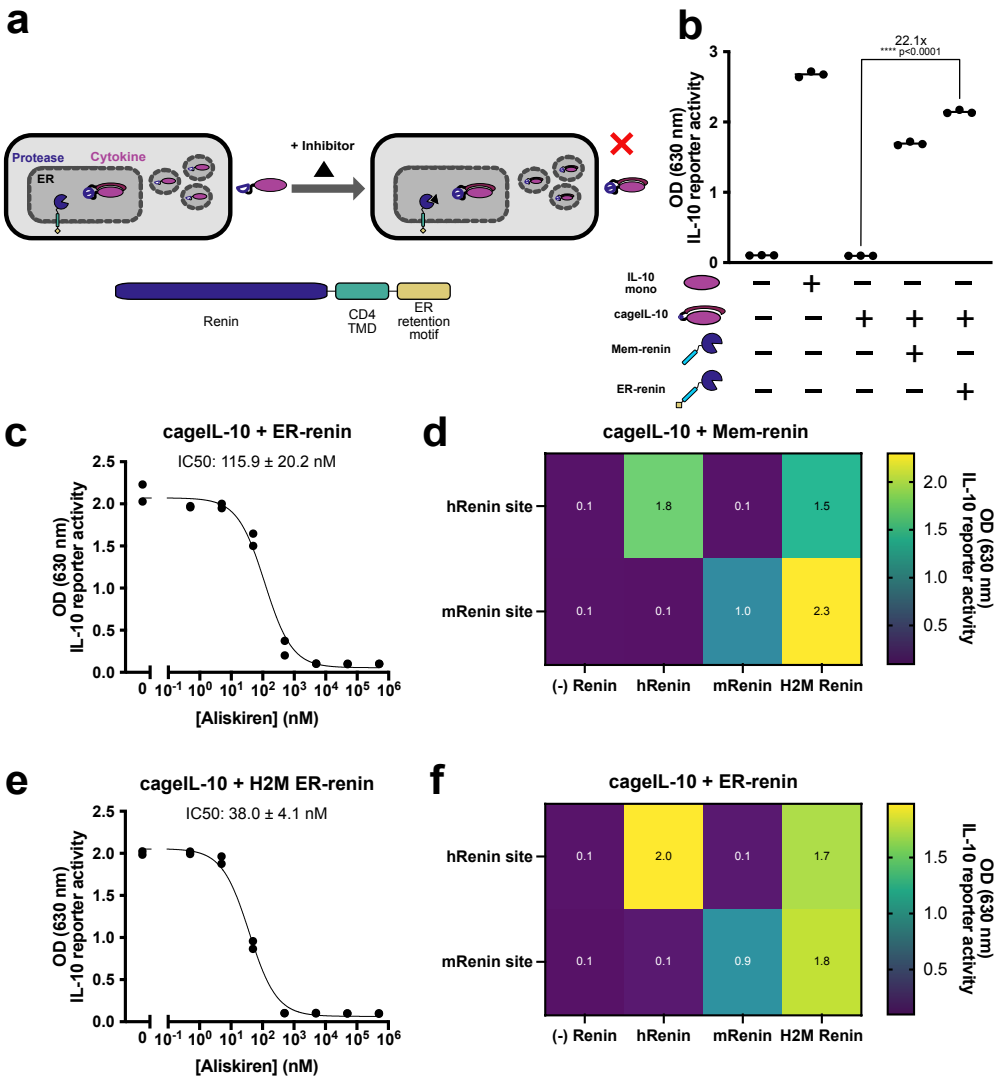

Fig. 4: Orthogonalization of renin. a, hDIRECT circuit using caged cytokines and ER-retained renin to control cytokine activity. Cells constitutively secrete caged cytokines and cytokine activity can be tuned via small-molecule inhibition of a co-expressed protease, renin. ER-renin is retained in ER via cytosolic motif and can cleave secreted cytokines. **b,** Activity of cageIL-10 transiently transfected with membrane (memRenin) or ER-retained (ER-renin) renin. **c,** Activity of cageIL-10 co-expressed with ER-renin at increasing aliskiren concentrations. **d,** Orthogonal renin matrix. Functional activity of cageIL-10 constructs containing human (h) or mouse (m) cut sites transiently transfected with membrane-bound human, mouse, or engineered H2M renin. **e,** Functional activity of cageIL-10 with an mRenin cut-site co-expressed with H2M ER-renin at increasing aliskiren concentrations. **f,** Orthogonal renin matrix. Functional activity of cageIL-10 constructs containing human (h) or mouse (m) cut sites transiently transfected with ER-retained human, mouse, or engineered H2M renin. Replicate data for **d,f** can be found in Supplementary Fig. 8. (Cytokine activity measured from supernatant using HEKBlue IL-10™ (**b-f**) reporter cells. For **b,d,f**: mean of n = 3 biological replicates; Individual replicate data for **d,f** can be found in Supplementary Fig. 5. Unpaired two-tailed Student's t-test. For **c,e**: n = 2 biological replicates; data represent mean ± s.e.m. **** $p < 0.0001$.)

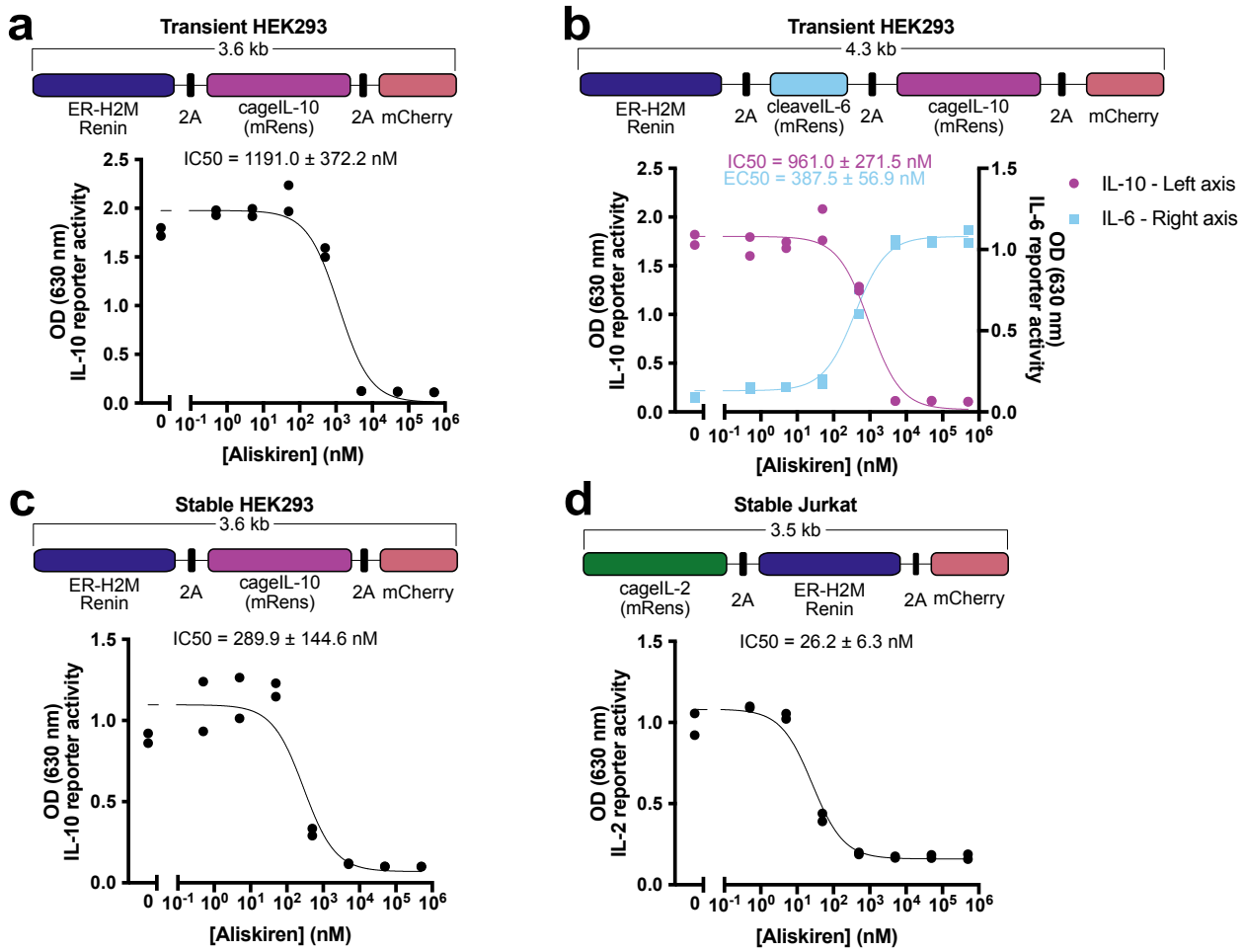

Fig. 5: Compact delivery of hDIRECT in mammalian cells. a, Polycistronic design of co-expressed cageIL-10 (mRens) and ER-H2M renin (top cartoon). Aliskerin-regulated activity of cageIL-10 in HEK293 cells transiently transfected with cageIL-10 single-transcript plasmid. **b,** Polycistronic design of cageIL-10 (mRens), cleaveIL-6 (mRens), and ER-H2M renin (top). Aliskiren-regulated activity of cageIL-10 (left-axis) and cleaveIL-6 (right-axis) in HEK293 cells transiently transfected with cageIL-10/cleaveIL-6 single-transcript plasmid. **c,** Aliskiren-regulated activity of cageIL-10 in HEK293 cells stably transduced with cageIL-10 single-transcript design (from **a**). **d,** Polycistronic design of co-expressed cageIL-2 (mRens) and ER-H2M renin (top cartoon). Aliskiren-regulated activity of cageIL-2 at increasing aliskiren concentrations from Jurkat cells stably transduced with cageIL-2 single-transcript design. (Cytokine activity measured from supernatant using HEKBlue IL-10™ (**a-c**), IL-6™ (**b**), and IL-2™ (**d**) reporter cells. For **a-d**: n = 2 biological replicates; data represent mean ± s.e.m.)

869

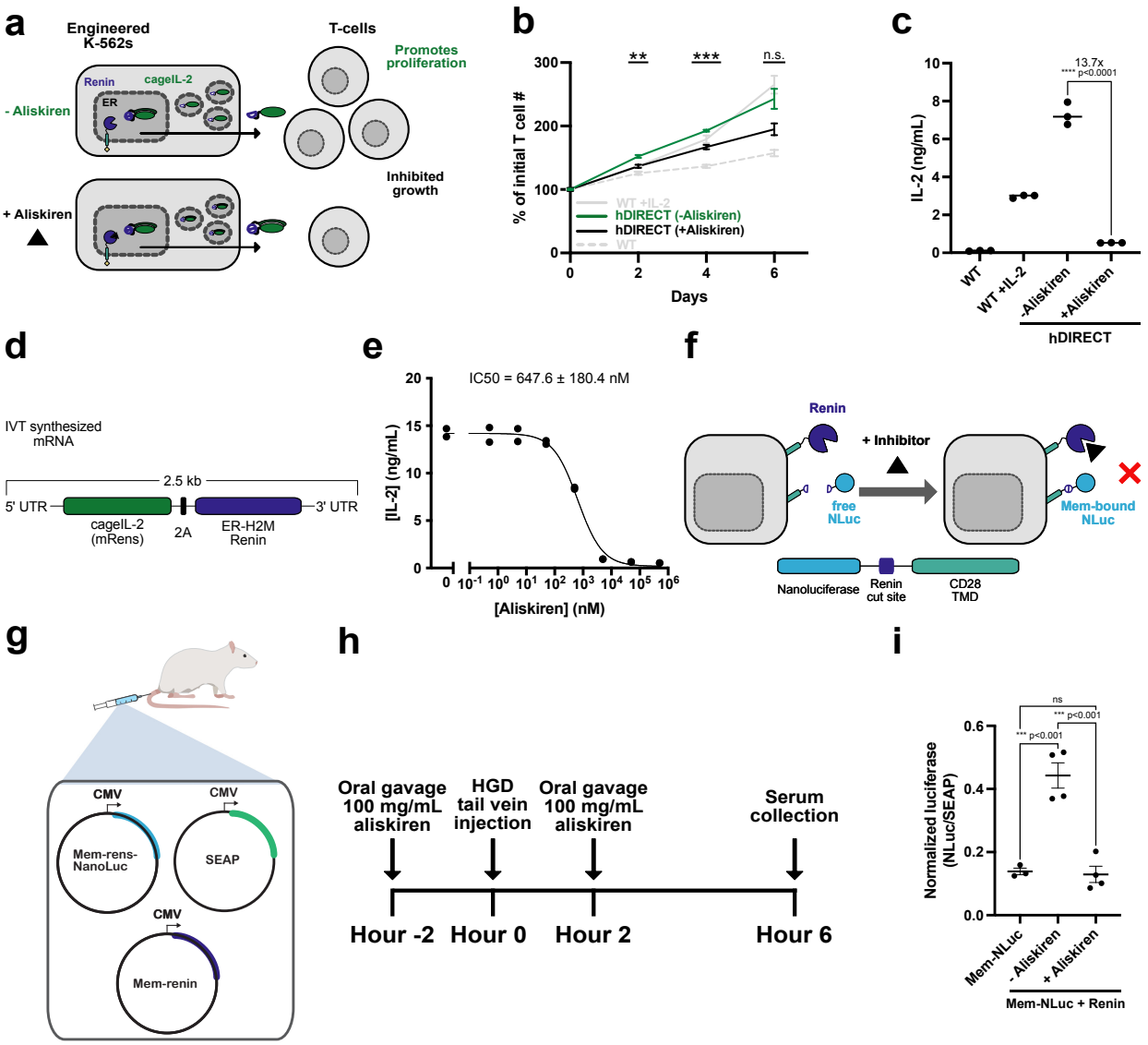
a
Engineered K-562s
T-cells
Promotes proliferation
Renin
cageIL-2
ER
- Aliskiren
+ Aliskiren
Inhibited growth
b
% of initial T cell #
Days
**
***
n.s.
WT +IL-2
hDIRECT (-Aliskiren)
hDIRECT (+Aliskiren)
WT
c
IL-2 (ng/mL)
13.7x
**** p<0.0001
WT
WT +IL-2
-Aliskiren
+Aliskiren
hDIRECT
d
IVT synthesized mRNA
2.5 kb
5' UTR
cageIL-2 (mRens)
2A
ER-H2M Renin
3' UTR
e
IC50 = 647.6 ± 180.4 nM
[IL-2] (ng/mL)
[Aliskiren] (nM)
f
Renin
+ Inhibitor
free NLuc
Mem-bound NLuc
Nanoluciferase
Renin cut site
CD28 TMD
g
CMV
Mem-rens-NanoLuc
SEAP
Mem-renin
h
Oral gavage 100 mg/mL aliskiren
HGD tail vein injection
Oral gavage 100 mg/mL aliskiren
Serum collection
Hour -2
Hour 0
Hour 2
Hour 6
i
Normalized luciferase (NLuc/SEAP)
ns
*** p<0.001
*** p<0.001
Mem-NLuc
- Aliskiren
+ Aliskiren
Mem-NLuc + Renin

870

Fig. 6: hDIRECT primary T cell proliferation co-culture. a, CageIL-2 hDIRECT circuit to control primary T cell proliferation using stably engineered K-562 cells via *in vitro* co-culture. **b,** Primary T cells were co-cultured with engineered K-562 cells (single-transcript lentivirus from Fig. 5d) in IL-2-free media at a 1:1 ratio. Cells were plated and induced with aliskiren (0 or 5000 nM) on Day 0 and live-cell counts were quantified via flow cytometry at the indicated days. Untransduced (wild-type) and cells supplemented with recombinant IL-2 (200 U/mL) were cultured and included as positive and negative controls. Asterisks represent p-values for t-tests between -Aliskiren and +Aliskiren conditions. **c,** Aliskiren-regulated IL-2 activity from stably engineered K-562 cells. Supernatant on Day 3 from T cell proliferation co-culture wells were assayed for IL-2 binding via ELISA. **d,** Single-transcript design of cageIL-2 hDIRECT circuit for mRNA delivery. **e,** Aliskerin-regulated level of cageIL-2 secreted from HEK293 cells transiently transfected with mRNA from (**d**) measured via IL-2 ELISA. **f,** hDIRECT circuit using membrane-bound nanoluciferase (NLuc) to control luciferase activity. Cells constitutively display NLuc on their surface which is cleaved free by renin. Luciferase activity can be tuned down via aliskiren. **g,** Testing exogenous renin's response to aliskiren *in vivo*. Cartoon of hydrodynamic gene delivery (HGD) of plasmids mice were given depending on condition. SEAP plasmid was used as a co-secretion factor to normalize total secretion. **h,** Timeline of *in vivo* mouse experiment, in which BALB/c mice were injected i.v. with plasmids via HGD. Mice were treated with 100 mg/kg of aliskiren or vehicle in two doses with oral gavage prior to and after plasmid delivery. Serum was collected to assay for target protein activity. **i,** Aliskiren-regulated activity of membrane-bound luciferase in mice. Serum was assayed for luminescence and normalized to SEAP activity. (For **b:** Lines represent mean values for n = 3 biological replicates ± SD. Significance was tested by unpaired two-tailed Student's t-test among multiple conditions with a Bonferroni correction for m = 3 conditions. * $p<0.0167$, ** $p<0.0033$, *** $p<0.0003$. For **c:** mean of n = 3 biological replicates. Unpaired two-tailed Student's t-test. **** $p<0.0001$. For **e:** n = 2 biological replicates; data represent mean ± s.e.m.. For **g:** error bars represent mean and standard deviation of n = 3 or 4 mice. One-way ANOVA with Tukey's multiple comparisons test. * $p<0.05$, *** $p<0.001$.)

871